EUROPEAN ORGANIZATION FOR NUCLEAR RESEARCH

CERN-EP/2000-118
August 28, 2000

Search for Charged Higgs Bosons in e^+e^- Collisions at Centre-of-Mass Energies up to 202 GeV

The L3 Collaboration

Abstract

A search for pair-produced charged Higgs bosons is performed with the L3 detector at LEP using data collected at centre-of-mass energies between 192 and 202 GeV, corresponding to an integrated luminosity of 233.2 pb^{-1}. Decays into a charm and a strange quark or into a tau lepton and its neutrino are considered. The observed events are consistent with the expectations from Standard Model background processes. Including data taken at lower centre-of-mass energies, lower limits on the charged Higgs mass are derived at the 95% confidence level. They vary from 67.4 to 79.9 GeV as a function of the $H^{\pm} \rightarrow \tau\nu$ branching ratio.

Submitted to *Phys. Lett. B*

Introduction

In the Standard Model [1], the Higgs mechanism [2] requires one doublet of complex scalar fields which leads to the prediction of a single neutral scalar Higgs boson. Extensions to the minimal Standard Model contain more than one Higgs doublet [3]. In particular, models with two complex Higgs doublets predict two charged Higgs bosons ($H^{\pm}$).

A search for the process $e^+e^- \rightarrow H^+H^-$ is performed in the three decay channels $H^+H^- \rightarrow \tau^+\nu_\tau\tau^-\bar{\nu}_\tau$, $H^+H^- \rightarrow c\bar{s}\tau^-\bar{\nu}_\tau$ [1)] and $H^+H^- \rightarrow c\bar{s}\bar{c}s$, assumed to be the only possible decays. This allows the interpretation of the results to be independent of the $H^{\pm} \rightarrow \tau\nu$ branching ratio.

The results in this letter are based on data collected at $\sqrt{s}$ between 191.6 and 201.7 GeV, as well as those from lower centre-of-mass energies, and supersede the previous lower limit on the mass of the charged Higgs boson established by L3 [4–6]. Results from other LEP experiments at lower centre-of-mass energies are given in Reference 7.

Data Analysis

The search for pair-produced charged Higgs bosons is performed using the data collected in 1999 with the L3 detector [8] at LEP, corresponding to an integrated luminosity of 233.2 pb^{-1}; where 29.7 pb^{-1} were collected at a centre-of-mass energy of 191.6 GeV, 83.7 pb^{-1} at 195.5 GeV, 82.8 pb^{-1} at 199.5 GeV and 37.0 pb^{-1} at 201.7 GeV. The analyses remain almost unchanged since our previous publications at centre-of-mass energies between 130 and 189 GeV [6,5], with the exception of the $c\bar{s}\bar{c}s$ final state which is described in more detail below.

The charged Higgs cross section is calculated using the HZHA Monte Carlo program [9]. For the efficiency estimates, samples of $e^+e^- \rightarrow H^+H^-$ events are generated with the PYTHIA Monte Carlo program [10] for Higgs masses between 50 and 95 GeV in mass steps of 5 GeV. About 1000 events for each final state are generated at each Higgs mass. For the background studies, the following Monte Carlo generators are used: PYTHIA for $e^+e^- \rightarrow q\bar{q}(\gamma)$, $e^+e^- \rightarrow ZZ$ and $e^+e^- \rightarrow Ze^+e^-$, KORALW [11] for $e^+e^- \rightarrow W^+W^-$, PHOJET [12] for $e^+e^- \rightarrow e^+e^-q\bar{q}$, DIAG36 [13] for $e^+e^- \rightarrow e^+e^-\ell^+\ell^-$ ($\ell = e, \mu, \tau$), KORALZ [14] for $e^+e^- \rightarrow \mu^+\mu^-$ and $e^+e^- \rightarrow \tau^+\tau^-$ and BHWIDE [15] for $e^+e^- \rightarrow e^+e^-$. The L3 detector response is simulated using the GEANT program [16] which takes into account the effects of energy loss, multiple scattering and showering in the detector. Time-dependent detector inefficiencies are taken into account in the simulation procedure.

As the theory does not predict the branching ratio for $H^{\pm} \rightarrow \tau\nu$, in the following the performance of each search channel is compared with a signal expectation for a value of $Br(H^{\pm} \rightarrow \tau\nu)$ which is most favourable for the corresponding channel. This performance is expected to be independent of the quark flavours in the hadronic decay.

Search in the $H^+H^- \rightarrow \tau^+\nu_\tau\tau^-\bar{\nu}_\tau$ channel

The signature for the leptonic decay channel is a pair of tau leptons with large missing energy and momentum, giving rise to low multiplicity events with low visible energy and a flat distribution in acollinearity, defined as the maximum angle between any pair of tracks. The performance of the analysis [6, 5] is not affected by the increased centre-of-mass energy, and

[1)] The charge conjugate reaction is implied throughout this letter.

Channel	Selection efficiency (%) for $m_{H^\pm}$ =				
	60 GeV	65 GeV	70 GeV	75 GeV	80 GeV
$\tau^+\nu_\tau\tau^-\bar{\nu}_\tau$	28	30	31	32	33
$c\bar{s}\tau^-\bar{\nu}_\tau$	42	42	43	41	37
$c\bar{s}\bar{c}s$	51	56	60	61	63

Table 1: The charged Higgs selection efficiencies for various Higgs masses, averaged over centre-of-mass energies and weighted with the luminosity. The efficiencies are almost independent of the centre-of-mass energy. The uncertainty on each efficiency is estimated to be 3%.

Channel	Centre-of-mass energy (GeV)				Total	
	191.6	195.5	199.5	201.7		
$\tau^+\nu_\tau\tau^-\bar{\nu}_\tau$	6	23	12	6	47	Data
	5.4	15.4	16.3	6.9	44.0	Background
$c\bar{s}\tau^-\bar{\nu}_\tau$	21	88	66	34	209	Data
	22.8	67.2	64.0	30.4	184.4	Background
$c\bar{s}\bar{c}s$	133	379	384	146	1042	Data
	139.1	384.9	364.6	162.5	1051.1	Background

Table 2: The number of data events and the background expectations per centre-of-mass energy. The uncertainty on the background expectations is estimated to be 6%.

the event selection remains unchanged. Figure 1 shows the distribution of the visible energy for events on which all other selection criteria are applied.

The efficiency of the $H^+H^- \rightarrow \tau^+\nu_\tau\tau^-\bar{\nu}_\tau$ selection for several Higgs masses is listed in Table 1. The number of data events and the background expectations are presented in Table 2 for the different centre-of-mass energies. Almost all the background comes from W-pair production. The number of events expected for a 70 GeV Higgs signal is 19.4 for $Br(H^\pm \rightarrow \tau\nu) = 1$.

Search in the $H^+H^- \rightarrow c\bar{s}\tau^-\bar{\nu}_\tau$ channel

The semileptonic final state $H^+H^- \rightarrow c\bar{s}\tau^-\bar{\nu}_\tau$ is characterised by two hadronic jets, a tau lepton and missing momentum. The selection criteria are the same as for the analysis performed at $\sqrt{s} = 189$ GeV [6].

The selection efficiencies are given in Table 1. The number of data events and the background expected from Standard Model processes are listed in Table 2 for the different centre-of-mass energies. The background is dominated by the process $W^+W^- \rightarrow q\bar{q}'\tau\nu$. The number of events expected for a 70 GeV Higgs signal is 13.2 for $Br(H^\pm \rightarrow \tau\nu) = 0.5$. Figure 2 displays the distribution of the average of the jet-jet and τ-ν masses. They are calculated from a kinematic fit imposing energy and momentum conservation for an assumed production of equal mass particles, keeping the directions of the jets, the tau and the missing momentum vector at their measured values.

Search in the $H^+H^- \to c\bar{s}\bar{c}s$ channel

Events from the $H^+H^- \to c\bar{s}\bar{c}s$ channel have a high multiplicity and are balanced in transverse and longitudinal momenta. A large fraction of the centre-of-mass energy is deposited in the detector, typically as four hadronic jets. The selection criteria are slightly modified with respect to the analysis at lower centre-of-mass energies [6,5], in order to gain sensitivity at higher masses.

Events with an identified electron, muon or photon with energy in excess of 65 GeV are discarded. A neural network [17] is applied to distinguish events with four genuine quark jets from those with two quark jets and two jets from gluon radiation. Further reduction of the QCD background is achieved by requiring the Durham jet resolution parameter, y_{34}, for which three-jet events are resolved into four-jet ones, to be greater than 0.003 and by requiring the minimum jet energy to exceed 6% of $\sqrt{s}$.

The charged Higgs production angle distribution has a $\sin^2\theta$ dependence, where θ is the polar angle with respect to the beam direction. A cut of $|\cos\theta| < 0.8$ is therefore applied to preferentially reject W-pair background.

The analysis of the 55.3 pb^{-1} and 176.4 pb^{-1} of data respectively taken at $\sqrt{s} = 183$ and 189 GeV is redone using the criteria described above, superseding the previous analysis [6, 5]. The number of events selected in data at these centre-of-mass energies is 1103, while 1085.7 background events are expected from Standard Model processes.

The selection efficiencies are listed in Table 1. The number of events selected in data and the background expectations are given in Table 2 for the different centre-of-mass energies. The main contribution to the background comes from W-pair decays into four jets. The number of events expected for a 70 GeV Higgs signal is 37.4 for $\text{Br}(H^\pm \to \tau\nu) = 0$. Figure 3 shows the dijet mass distribution after a kinematic fit imposing four-momentum conservation and equal dijet masses. A slight excess is observed around 68 GeV.

Results

The number of selected events in each decay channel is consistent with the number of events expected from Standard Model processes. However, there is an excess of events in the $c\bar{s}\bar{c}s$ and $c\bar{s}\tau^-\bar{\nu}_\tau$ mass distributions around 68 GeV. Figure 4 displays the combined background-subtracted mass distribution for these two Higgs decay channels, where the events are corrected for the efficiency of their respective analyses. The figure also shows the expected distribution for a 68 GeV Higgs with $\text{Br}(H^\pm \to \tau\nu) = 0.1$. This value of the $\text{Br}(H^\pm \to \tau\nu)$ is in the range of branching fractions for which the observed excess of events is closest to the expected number for a 68 GeV mass Higgs, as is described in more detail below.

In order to estimate the significance of this excess, the systematic errors on the background and signal efficiencies are taken into account. The main systematic uncertainties come from the finite Monte Carlo statistics and the precision of the cross sections for the background processes. The former is calculated for each final state using binomial statistics, leading to an overall 5% uncertainty in the background and 3% in the signal normalisation. The latter affects the analyses in different ways depending on the background composition. This uncertainty is 2% for the $H^+H^- \to \tau^+\nu_\tau\tau^-\bar{\nu}_\tau$ and $c\bar{s}\tau^-\bar{\nu}_\tau$ channels, and 3% for $c\bar{s}\bar{c}s$. The systematic uncertainty on the signal efficiency due to the selection is estimated to be less than 1%, by varying the cut values. The total systematic error on the number of expected background and signal events is therefore estimated to be 6% and 3%, respectively.

A technique based on a log-likelihood ratio [18] is used to calculate a confidence level

$\mathrm{Br}(\mathrm{H}^\pm \to \tau\nu)$	Lower limits at 95% CL (GeV) observed	median expected
0.0	76.5	75.9
0.1	67.4	74.9
0.5	70.5	73.8
1.0	79.9	79.2

Table 3: Observed and median expected lower limits at 95% CL for different values of the $\mathrm{H}^\pm \to \tau\nu$ branching ratio. The minimum observed limit, independent of the branching fraction, is at $\mathrm{Br}(\mathrm{H}^\pm \to \tau\nu) = 0.1$.

(CL) that the observed events are consistent with background expectations. The test-statistic adopted, Q, is the ratio of the likelihood function for the signal plus background hypothesis to the likelihood function for the background only hypothesis. For the $\mathrm{c\bar{s}\bar{c}s}$ and $\mathrm{c\bar{s}}\tau^-\bar{\nu}_\tau$ channels, the reconstructed mass distributions (Figures 2 and 3) are used in the calculation, whereas for the $\tau^+\nu_\tau\tau^-\bar{\nu}_\tau$ channel, the total number of data, expected background and expected signal events are used. The systematic uncertainties on the background and signal efficiencies are included in the confidence level calculation.

Figure 5 shows the resulting negative log-likelihood ratio, $-2\ln(Q)$, using $\mathrm{Br}(\mathrm{H}^\pm \to \tau\nu) = 0.1$, as a function of the Higgs mass, for the data and for the expectation in the absence of a signal. The one and two standard deviation (σ) probability bands expected in the absence of a signal are also displayed. The excess of events around $m_{\mathrm{H}^\pm} = 68$ GeV is compatible with a 2.7σ fluctuation in the background. The statistical significance of the excess is almost constant for values of $\mathrm{Br}(\mathrm{H}^\pm \to \tau\nu)$ between 0.1 and 0.2. Figure 5 also shows the expected $-2\ln(Q)$ distribution for the hypothesis of a 68 GeV mass Higgs signal and its 1σ under-fluctuation. The data are 1.4σ below what is expected for a Higgs signal at this mass. Again, this difference is not strongly dependent on the value of the branching fraction.

Interpreting this excess as a statistical fluctuation in the background, lower limits on the charged Higgs mass as a function of the $\mathrm{Br}(\mathrm{H}^\pm \to \tau\nu)$ are derived [18,19] at the 95% CL, using the data from $\sqrt{s}$ between 191.6 and 201.7 GeV, as well as those from lower centre-of-mass energies [6,5]. Figure 6 shows the excluded Higgs mass regions for each of the final states and their combination, as a function of the $\mathrm{Br}(\mathrm{H}^\pm \to \tau\nu)$. Some regions which are excluded using one channel are not excluded when all three channels are combined. Table 3 gives the observed and the median expected lower limits for several values of the branching ratio. The region around $m_{\mathrm{H}^\pm} = 68$ GeV at low values of the $\mathrm{Br}(\mathrm{H}^\pm \to \tau\nu)$ can only be excluded at 88% CL, due to the aforementioned excess of events in this mass region. A similar but less significant excess was observed in our previous publication [6].

Our sensitivity to larger Higgs masses, as quantified by the median expected mass limits given in Table 3, is significantly improved as compared with our previous results at lower centre-of-mass energies [6,5]. Combining all our data, we obtain a new lower limit at 95% CL of

$$m_{\mathrm{H}^\pm} > 67.4 \text{ GeV},$$

independent of the branching ratio.

Acknowledgements

We wish to express our gratitude to the CERN accelerator divisions for the excellent performance of the LEP machine. We acknowledge the contributions of the engineers and technicians who have participated in the construction and maintenance of this experiment.

References

[1] S.L. Glashow, Nucl. Phys. **22** (1961) 579;
S. Weinberg, Phys. Rev. Lett. **19** (1967) 1264;
A. Salam, *Elementary Particle Theory*, edited by N. Svartholm (Almqvist and Wiksell, Stockholm, 1968), p. 367.

[2] P.W. Higgs, Phys. Lett. **12** (1964) 132, Phys. Rev. Lett. **13** (1964) 508 and Phys. Rev. **145** (1966) 1156;
F. Englert and R. Brout, Phys. Rev. Lett. **13** (1964) 321;
G.S. Guralnik, C.R. Hagen and T.W.B. Kibble, Phys. Rev. Lett. **13** (1964) 585.

[3] S. Dawson *et al.*, *The Physics of the Higgs Bosons: Higgs Hunter's Guide*, Addison Wesley, Menlo Park, 1989.

[4] L3 Collab., O. Adriani *et al.*, Phys. Lett. **B 294** (1992) 457;
L3 Collab., O. Adriani *et al.*, Z. Phys. **C 57** (1993) 355.

[5] L3 Collab., M. Acciarri *et al.*, Phys. Lett. **B 446** (1999) 368.

[6] L3 Collab., M. Acciarri *et al.*, Phys. Lett. **B 466** (1999) 71.

[7] ALEPH Collab., R. Barate *et al.*, Phys. Lett. **B 418** (1998) 419;
ALEPH Collab., R. Barate *et al.*, Phys. Lett. **B 450** (1999) 467;
DELPHI Collab., P. Abreu *et al.*, Phys. Lett. **B 420** (1998) 140;
OPAL Collab., K. Ackerstaff *et al.*, Phys. Lett. **B 426** (1998) 180;
OPAL Collab., G. Abbiendi *et al.*, Eur. Phys. J. **C 7** (1999) 407.

[8] L3 Collab., B. Adeva *et al.*, Nucl. Instr. Meth. **A 289** (1990) 35;
J.A. Bakken *et al.*, Nucl. Instr. Meth. **A 275** (1989) 81;
O. Adriani *et al.*, Nucl. Instr. Meth. **A 302** (1991) 53;
B. Adeva *et al.*, Nucl. Instr. Meth. **A 323** (1992) 109;
K. Deiters *et al.*, Nucl. Instr. Meth. **A 323** (1992) 162;
M. Chemarin *et al.*, Nucl. Instr. Meth. **A 349** (1994) 345;
M. Acciarri *et al.*, Nucl. Instr. Meth. **A 351** (1994) 300;
G. Basti *et al.*, Nucl. Instr. Meth. **A 374** (1996) 293;
A. Adam *et al.*, Nucl. Instr. Meth. **A 383** (1996) 342;
O. Adriani *et al.*, Phys. Rep. **236** (1993) 1.

[9] HZHA version 2 is used. P. Janot, in *Physics at LEP2*, ed. G. Altarelli, T. Sjöstrand and F. Zwirner, (CERN 96-01, 1996), volume 2, p. 309.

[10] T. Sjöstrand, CERN-TH 7112/93, CERN (1993), revised August 1995;
T. Sjöstrand, Comp. Phys. Comm. **82** (1994) 74.

[11] M. Skrzypek *et al.*, Comp. Phys. Comm. **94** (1996) 216;
M. Skrzypek *et al.*, Phys. Lett. **B 372** (1996) 289.

[12] R. Engel, Z. Phys. **C 66** (1995) 203;
R. Engel and J. Ranft, Phys. Rev. **D 54** (1996) 4244.

[13] F.A. Berends, P.H. Daverfeldt and R. Kleiss, Nucl. Phys. **B 253** (1985) 441.

[14] S. Jadach, B.F.L. Ward and Z. Wąs, Comp. Phys. Comm. **79** (1994) 503.

[15] S. Jadach *et al.*, Phys. Lett. **B 390** (1997) 298.

[16] R. Brun *et al.*, *GEANT 3*, CERN DD/EE/84-1 (Revised), September 1987.
The GHEISHA program (H. Fesefeldt, RWTH Aachen Report PITHA 85/02, 1985) is used to simulate hadronic interactions.

[17] L3 Collab., M. Acciarri *et al.*, Preprint CERN-EP/2000-104.

[18] ALEPH, DELPHI, L3 and OPAL Collab., The LEP Working Group for Higgs Boson Searches, Preprint CERN-EP/2000-055.

[19] L3 Collab., O. Adriani *et al.*, Phys. Lett. **B 411** (1997) 373.

The L3 Collaboration:

M.Acciarri,[26] P.Achard,[19] O.Adriani,[16] M.Aguilar-Benitez,[25] J.Alcaraz,[25] G.Alemanni,[22] J.Allaby,[17] A.Aloisio,[28] M.G.Alviggi,[28] G.Ambrosi,[19] H.Anderhub,[48] V.P.Andreev,[6,36] T.Angelescu,[12] F.Anselmo,[9] A.Arefiev,[27] T.Azemoon,[3] T.Aziz,[10] P.Bagnaia,[35] A.Bajo,[25] L.Baksay,[43] A.Balandras,[4] S.V.Baldew,[2] S.Banerjee,[10] Sw.Banerjee,[10] A.Barczyk,[48,46] R.Barillère,[17] P.Bartalini,[22] M.Basile,[9] R.Battiston,[32] A.Bay,[22] F.Becattini,[16] U.Becker,[14] F.Behner,[48] L.Bellucci,[16] R.Berbeco,[3] J.Berdugo,[25] P.Berges,[14] B.Bertucci,[32] B.L.Betev,[48] S.Bhattacharya,[10] M.Biasini,[32] A.Biland,[48] J.J.Blaising,[4] S.C.Blyth,[33] G.J.Bobbink,[2] A.Böhm,[1] L.Boldizsar,[13] B.Borgia,[35] D.Bourilkov,[48] M.Bourquin,[19] S.Braccini,[19] J.G.Branson,[39] F.Brochu,[4] A.Buffini,[16] A.Buijs,[44] J.D.Burger,[14] W.J.Burger,[32] X.D.Cai,[14] M.Capell,[14] G.Cara Romeo,[9] G.Carlino,[28] A.M.Cartacci,[16] J.Casaus,[25] G.Castellini,[16] F.Cavallari,[35] N.Cavallo,[37] C.Cecchi,[32] M.Cerrada,[25] F.Cesaroni,[23] M.Chamizo,[19] Y.H.Chang,[50] U.K.Chaturvedi,[18] M.Chemarin,[24] A.Chen,[50] G.Chen,[7] G.M.Chen,[7] H.F.Chen,[20] H.S.Chen,[7] G.Chiefari,[28] L.Cifarelli,[38] F.Cindolo,[9] C.Civinini,[16] I.Clare,[14] R.Clare,[14] G.Coignet,[4] N.Colino,[25] S.Costantini,[5] F.Cotorobai,[12] B.de la Cruz,[25] A.Csilling,[13] S.Cucciarelli,[32] T.S.Dai,[14] J.A.van Dalen,[30] R.D'Alessandro,[16] R.de Asmundis,[28] P.Déglon,[19] A.Degré,[4] K.Deiters,[46] D.della Volpe,[28] E.Delmeire,[19] P.Denes,[34] F.DeNotaristefani,[35] A.De Salvo,[48] M.Diemoz,[35] M.Dierckxsens,[2] D.van Dierendonck,[2] C.Dionisi,[35] M.Dittmar,[48] A.Dominguez,[39] A.Doria,[28] M.T.Dova,[18,♯] D.Duchesneau,[4] D.Dufournaud,[4] P.Duinker,[2] I.Duran,[40] H.El Mamouni,[24] A.Engler,[33] F.J.Eppling,[14] F.C.Erné,[2] P.Extermann,[19] M.Fabre,[46] M.A.Falagan,[25] S.Falciano,[35,17] A.Favara,[17] J.Fay,[24] O.Fedin,[36] M.Felcini,[48] T.Ferguson,[33] H.Fesefeldt,[1] E.Fiandrini,[32] J.H.Field,[19] F.Filthaut,[17] P.H.Fisher,[14] I.Fisk,[39] G.Forconi,[14] K.Freudenreich,[48] C.Furetta,[26] Yu.Galaktionov,[27,14] S.N.Ganguli,[10] P.Garcia-Abia,[5] M.Gataullin,[31] S.S.Gau,[11] S.Gentile,[35,17] N.Gheordanescu,[12] S.Giagu,[35] Z.F.Gong,[20] G.Grenier,[24] O.Grimm,[48] M.W.Gruenewald,[8] M.Guida,[38] R.van Gulik,[2] V.K.Gupta,[34] A.Gurtu,[10] L.J.Gutay,[45] D.Haas,[5] A.Hasan,[29] D.Hatzifotiadou,[9] T.Hebbeker,[8] A.Hervé,[17] P.Hidas,[13] J.Hirschfelder,[33] H.Hofer,[48] G. Holzner,[48] H.Hoorani,[33] S.R.Hou,[50] Y.Hu,[30] I.Iashvili,[47] B.N.Jin,[7] L.W.Jones,[3] P.de Jong,[2] I.Josa-Mutuberría,[25] R.A.Khan,[18] M.Kaur,[18,◇] M.N.Kienzle-Focacci,[19] D.Kim,[35] J.K.Kim,[42] J.Kirkby,[17] D.Kiss,[13] W.Kittel,[30] A.Klimentov,[14,27] A.C.König,[30] A.Kopp,[47] V.Koutsenko,[14,27] M.Kräber,[48] R.W.Kraemer,[33] W.Krenz,[1] A.Krüger,[47] A.Kunin,[14,27] P.Ladron de Guevara,[25] I.Laktineh,[24] G.Landi,[16] M.Lebeau,[17] A.Lebedev,[14] P.Lebrun,[24] P.Lecomte,[48] P.Lecoq,[17] P.Le Coultre,[48] H.J.Lee,[8] J.M.Le Goff,[17] R.Leiste,[47] P.Levtchenko,[36] C.Li,[20] S.Likhoded,[47] C.H.Lin,[50] W.T.Lin,[50] F.L.Linde,[2] L.Lista,[28] Z.A.Liu,[7] W.Lohmann,[47] E.Longo,[35] Y.S.Lu,[7] K.Lübelsmeyer,[1] C.Luci,[17,35] D.Luckey,[14] L.Lugnier,[24] L.Luminari,[35] W.Lustermann,[48] W.G.Ma,[20] M.Maity,[10] L.Malgeri,[17] A.Malinin,[17] C.Maña,[25] D.Mangeol,[30] J.Mans,[34] G.Marian,[15] J.P.Martin,[24] F.Marzano,[35] K.Mazumdar,[10] R.R.McNeil,[6] S.Mele,[17] L.Merola,[28] M.Meschini,[16] W.J.Metzger,[30] M.von der Mey,[1] A.Mihul,[12] H.Milcent,[17] G.Mirabelli,[35] J.Mnich,[17] G.B.Mohanty,[10] T.Moulik,[10] G.S.Muanza,[24] A.J.M.Muijs,[2] B.Musicar,[39] M.Musy,[35] M.Napolitano,[28] F.Nessi-Tedaldi,[48] H.Newman,[31] T.Niessen,[1] A.Nisati,[35] H.Nowak,[47] R.Ofierzynski,[48] G.Organtini,[35] A.Oulianov,[27] C.Palomares,[25] D.Pandoulas,[1] S.Paoletti,[35,17] P.Paolucci,[28] R.Paramatti,[35] H.K.Park,[33] I.H.Park,[42] G.Passaleva,[17] S.Patricelli,[28] T.Paul,[11] M.Pauluzzi,[32] C.Paus,[17] F.Pauss,[48] M.Pedace,[35] S.Pensotti,[26] D.Perret-Gallix,[4] B.Petersen,[30] D.Piccolo,[28] F.Pierella,[9] M.Pieri,[16] P.A.Piroué,[34] E.Pistolesi,[26] V.Plyaskin,[27] M.Pohl,[19] V.Pojidaev,[27,16] H.Postema,[14] J.Pothier,[17] D.O.Prokofiev,[45] D.Prokofiev,[36] J.Quartieri,[38] G.Rahal-Callot,[48,17] M.A.Rahaman,[10] P.Raics,[15] N.Raja,[10] R.Ramelli,[48] P.G.Rancoita,[26] R.Ranieri,[16] A.Raspereza,[47] G.Raven,[39] P.Razis,[29] D.Ren,[48] M.Rescigno,[35] S.Reucroft,[11] S.Riemann,[47] K.Riles,[3] J.Rodin,[43] B.P.Roe,[3] L.Romero,[25] A.Rosca,[8] S.Rosier-Lees,[4] J.A.Rubio,[17] G.Ruggiero,[16] H.Rykaczewski,[48] S.Saremi,[6] S.Sarkar,[35] J.Salicio,[17] E.Sanchez,[17] M.P.Sanders,[30] M.E.Sarakinos,[21] C.Schäfer,[17] V.Schegelsky,[36] S.Schmidt-Kaerst,[1] D.Schmitz,[1] H.Schopper,[49] D.J.Schotanus,[30] G.Schwering,[1] C.Sciacca,[28] A.Seganti,[9] L.Servoli,[32] S.Shevchenko,[31] N.Shivarov,[41] V.Shoutko,[27] E.Shumilov,[27] A.Shvorob,[31] T.Siedenburg,[1] D.Son,[42] B.Smith,[33] P.Spillantini,[16] M.Steuer,[14] D.P.Stickland,[34] A.Stone,[6] B.Stoyanov,[41] A.Straessner,[1] K.Sudhakar,[10] G.Sultanov,[18] L.Z.Sun,[20] H.Suter,[48] J.D.Swain,[18] Z.Szillasi,[43,¶] T.Sztaricskai,[43,¶] X.W.Tang,[7] L.Tauscher,[5] L.Taylor,[11] B.Tellili,[24] C.Timmermans,[30] Samuel C.C.Ting,[14] S.M.Ting,[14] S.C.Tonwar,[10] J.Tóth,[13] C.Tully,[17] K.L.Tung,[7] Y.Uchida,[14] J.Ulbricht,[48] E.Valente,[35] G.Vesztergombi,[13] I.Vetlitsky,[27] D.Vicinanza,[38] G.Viertel,[48] S.Villa,[11] M.Vivargent,[4] S.Vlachos,[5] I.Vodopianov,[36] H.Vogel,[33] H.Vogt,[47] I.Vorobiev,[27] A.A.Vorobyov,[36] A.Vorvolakos,[29] M.Wadhwa,[5] W.Wallraff,[1] M.Wang,[14] X.L.Wang,[20] Z.M.Wang,[20] A.Weber,[1] M.Weber,[1] P.Wienemann,[1] H.Wilkens,[30] S.X.Wu,[14] S.Wynhoff,[17] L.Xia,[31] Z.Z.Xu,[20] J.Yamamoto,[3] B.Z.Yang,[20] C.G.Yang,[7] H.J.Yang,[7] M.Yang,[7] J.B.Ye,[20] S.C.Yeh,[51] An.Zalite,[36] Yu.Zalite,[36] Z.P.Zhang,[20] G.Y.Zhu,[7] R.Y.Zhu,[31] A.Zichichi,[9,17,18] G.Zilizi,[43,¶] B.Zimmermann,[48] M.Zöller.[1]

1 I. Physikalisches Institut, RWTH, D-52056 Aachen, FRG§
III. Physikalisches Institut, RWTH, D-52056 Aachen, FRG§
2 National Institute for High Energy Physics, NIKHEF, and University of Amsterdam, NL-1009 DB Amsterdam, The Netherlands
3 University of Michigan, Ann Arbor, MI 48109, USA
4 Laboratoire d'Annecy-le-Vieux de Physique des Particules, LAPP,IN2P3-CNRS, BP 110, F-74941 Annecy-le-Vieux CEDEX, France
5 Institute of Physics, University of Basel, CH-4056 Basel, Switzerland
6 Louisiana State University, Baton Rouge, LA 70803, USA
7 Institute of High Energy Physics, IHEP, 100039 Beijing, China△
8 Humboldt University, D-10099 Berlin, FRG§
9 University of Bologna and INFN-Sezione di Bologna, I-40126 Bologna, Italy
10 Tata Institute of Fundamental Research, Bombay 400 005, India
11 Northeastern University, Boston, MA 02115, USA
12 Institute of Atomic Physics and University of Bucharest, R-76900 Bucharest, Romania
13 Central Research Institute for Physics of the Hungarian Academy of Sciences, H-1525 Budapest 114, Hungary‡
14 Massachusetts Institute of Technology, Cambridge, MA 02139, USA
15 KLTE-ATOMKI, H-4010 Debrecen, Hungary¶
16 INFN Sezione di Firenze and University of Florence, I-50125 Florence, Italy
17 European Laboratory for Particle Physics, CERN, CH-1211 Geneva 23, Switzerland
18 World Laboratory, FBLJA Project, CH-1211 Geneva 23, Switzerland
19 University of Geneva, CH-1211 Geneva 4, Switzerland
20 Chinese University of Science and Technology, USTC, Hefei, Anhui 230 029, China△
21 SEFT, Research Institute for High Energy Physics, P.O. Box 9, SF-00014 Helsinki, Finland
22 University of Lausanne, CH-1015 Lausanne, Switzerland
23 INFN-Sezione di Lecce and Universitá Degli Studi di Lecce, I-73100 Lecce, Italy
24 Institut de Physique Nucléaire de Lyon, IN2P3-CNRS,Université Claude Bernard, F-69622 Villeurbanne, France
25 Centro de Investigaciones Energéticas, Medioambientales y Tecnologícas, CIEMAT, E-28040 Madrid, Spain♭
26 INFN-Sezione di Milano, I-20133 Milan, Italy
27 Institute of Theoretical and Experimental Physics, ITEP, Moscow, Russia
28 INFN-Sezione di Napoli and University of Naples, I-80125 Naples, Italy
29 Department of Natural Sciences, University of Cyprus, Nicosia, Cyprus
30 University of Nijmegen and NIKHEF, NL-6525 ED Nijmegen, The Netherlands
31 California Institute of Technology, Pasadena, CA 91125, USA
32 INFN-Sezione di Perugia and Universitá Degli Studi di Perugia, I-06100 Perugia, Italy
33 Carnegie Mellon University, Pittsburgh, PA 15213, USA
34 Princeton University, Princeton, NJ 08544, USA
35 INFN-Sezione di Roma and University of Rome, "La Sapienza", I-00185 Rome, Italy
36 Nuclear Physics Institute, St. Petersburg, Russia
37 INFN-Sezione di Napoli and University of Potenza, I-85100 Potenza, Italy
38 University and INFN, Salerno, I-84100 Salerno, Italy
39 University of California, San Diego, CA 92093, USA
40 Dept. de Fisica de Particulas Elementales, Univ. de Santiago, E-15706 Santiago de Compostela, Spain
41 Bulgarian Academy of Sciences, Central Lab. of Mechatronics and Instrumentation, BU-1113 Sofia, Bulgaria
42 Laboratory of High Energy Physics, Kyungpook National University, 702-701 Taegu, Republic of Korea
43 University of Alabama, Tuscaloosa, AL 35486, USA
44 Utrecht University and NIKHEF, NL-3584 CB Utrecht, The Netherlands
45 Purdue University, West Lafayette, IN 47907, USA
46 Paul Scherrer Institut, PSI, CH-5232 Villigen, Switzerland
47 DESY, D-15738 Zeuthen, FRG
48 Eidgenössische Technische Hochschule, ETH Zürich, CH-8093 Zürich, Switzerland
49 University of Hamburg, D-22761 Hamburg, FRG
50 National Central University, Chung-Li, Taiwan, China
51 Department of Physics, National Tsing Hua University, Taiwan, China
§ Supported by the German Bundesministerium für Bildung, Wissenschaft, Forschung und Technologie
‡ Supported by the Hungarian OTKA fund under contract numbers T019181, F023259 and T024011.
¶ Also supported by the Hungarian OTKA fund under contract numbers T22238 and T026178.
♭ Supported also by the Comisión Interministerial de Ciencia y Tecnología.
♯ Also supported by CONICET and Universidad Nacional de La Plata, CC 67, 1900 La Plata, Argentina.
♢ Also supported by Panjab University, Chandigarh-160014, India.
△ Supported by the National Natural Science Foundation of China.

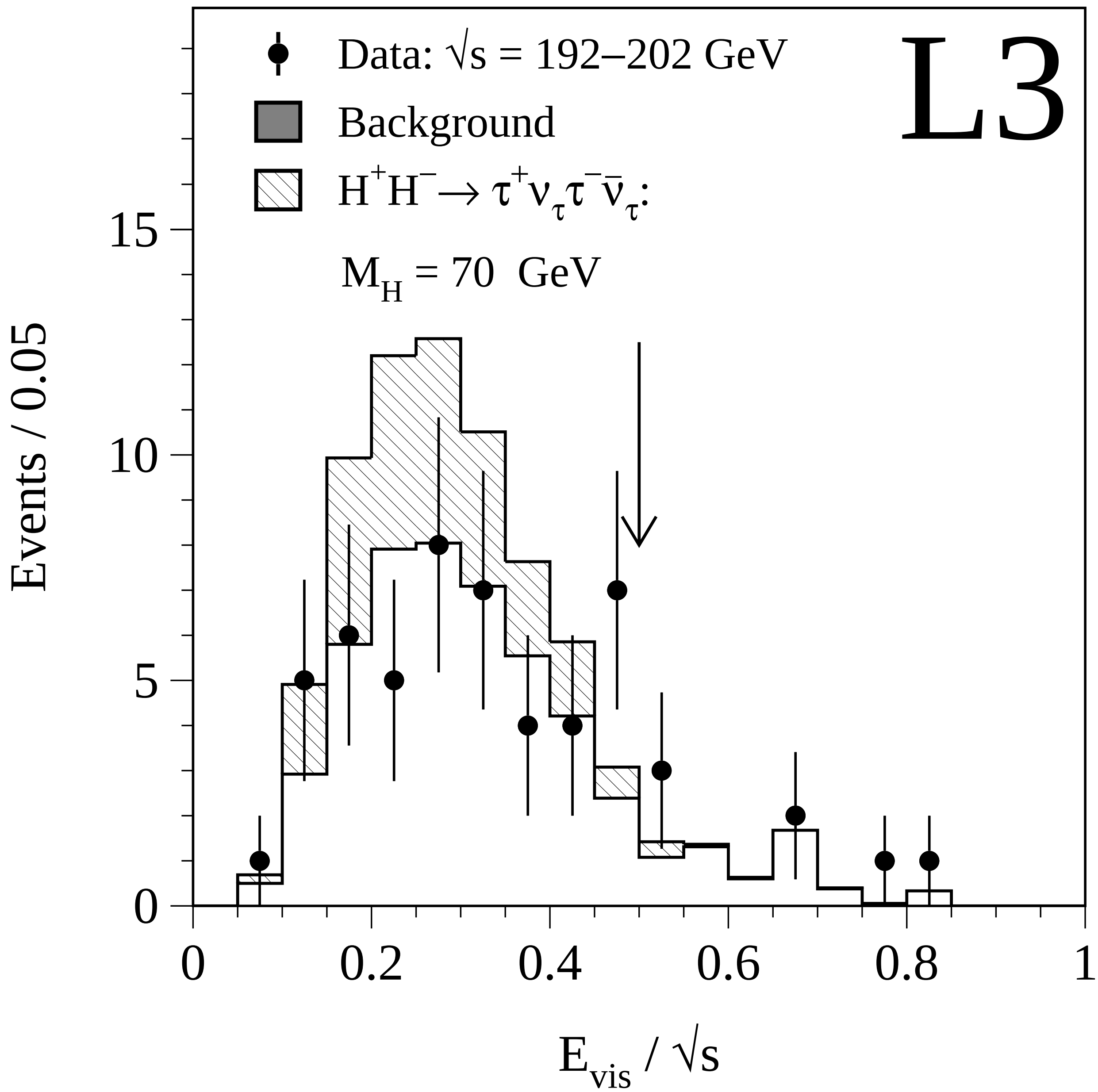

Figure 1: Distribution of the normalised visible energy, $E_{vis}/\sqrt{s}$, for the $H^+H^- \rightarrow \tau^+\nu_\tau\tau^-\bar{\nu}_\tau$ channel after all other cuts are applied. The arrow shows the cut position. The hatched histogram indicates the expected distribution for a 70 GeV Higgs with $Br(H^\pm \rightarrow \tau\nu) = 1$.

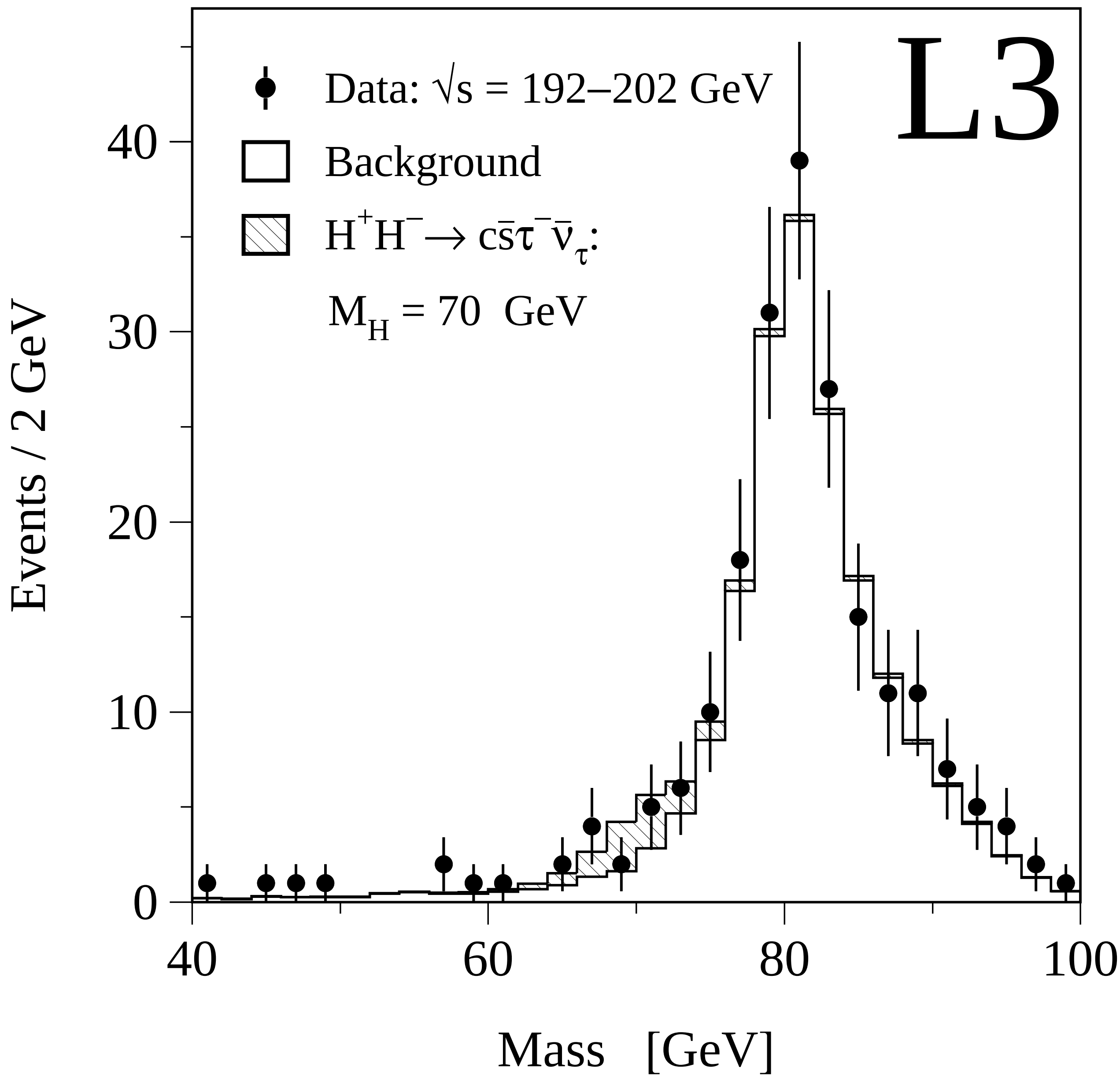

Figure 2: Reconstructed mass spectrum for data and expected background in the $H^+H^- \rightarrow c\bar{s}\tau^-\bar{\nu}_\tau$ channel. The expected distribution for a 70 GeV Higgs with $Br(H^\pm \rightarrow \tau\nu) = 0.5$ is added as the hatched histogram.

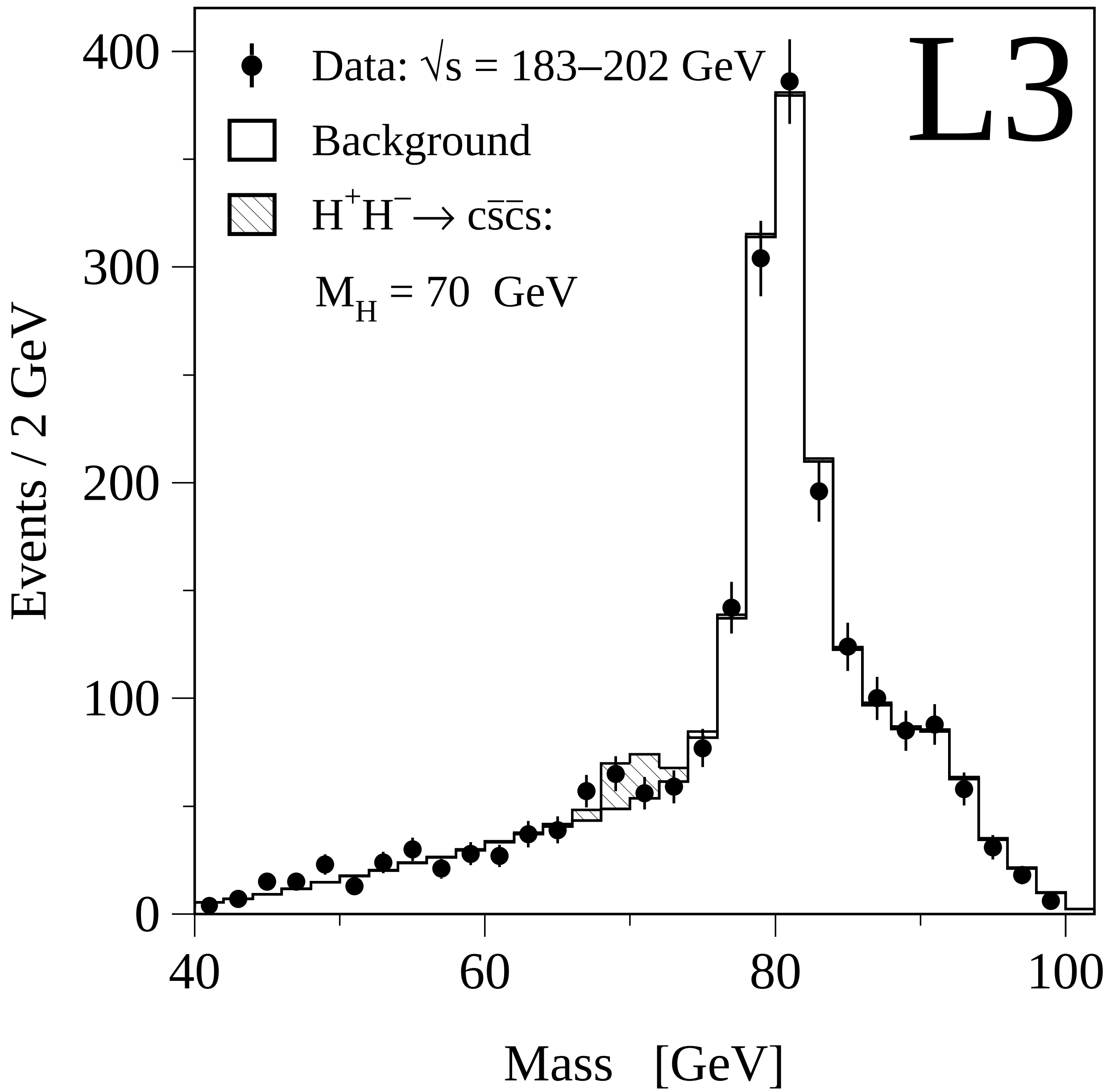

Figure 3: Distribution of the mass resulting from a kinematic fit, assuming production of equal mass particles, for data and expected background in the $H^+H^- \rightarrow c\bar{s}\bar{c}s$ channel. The hatched histogram indicates the expected distribution for a 70 GeV Higgs with $Br(H^\pm \rightarrow \tau\nu) = 0$.

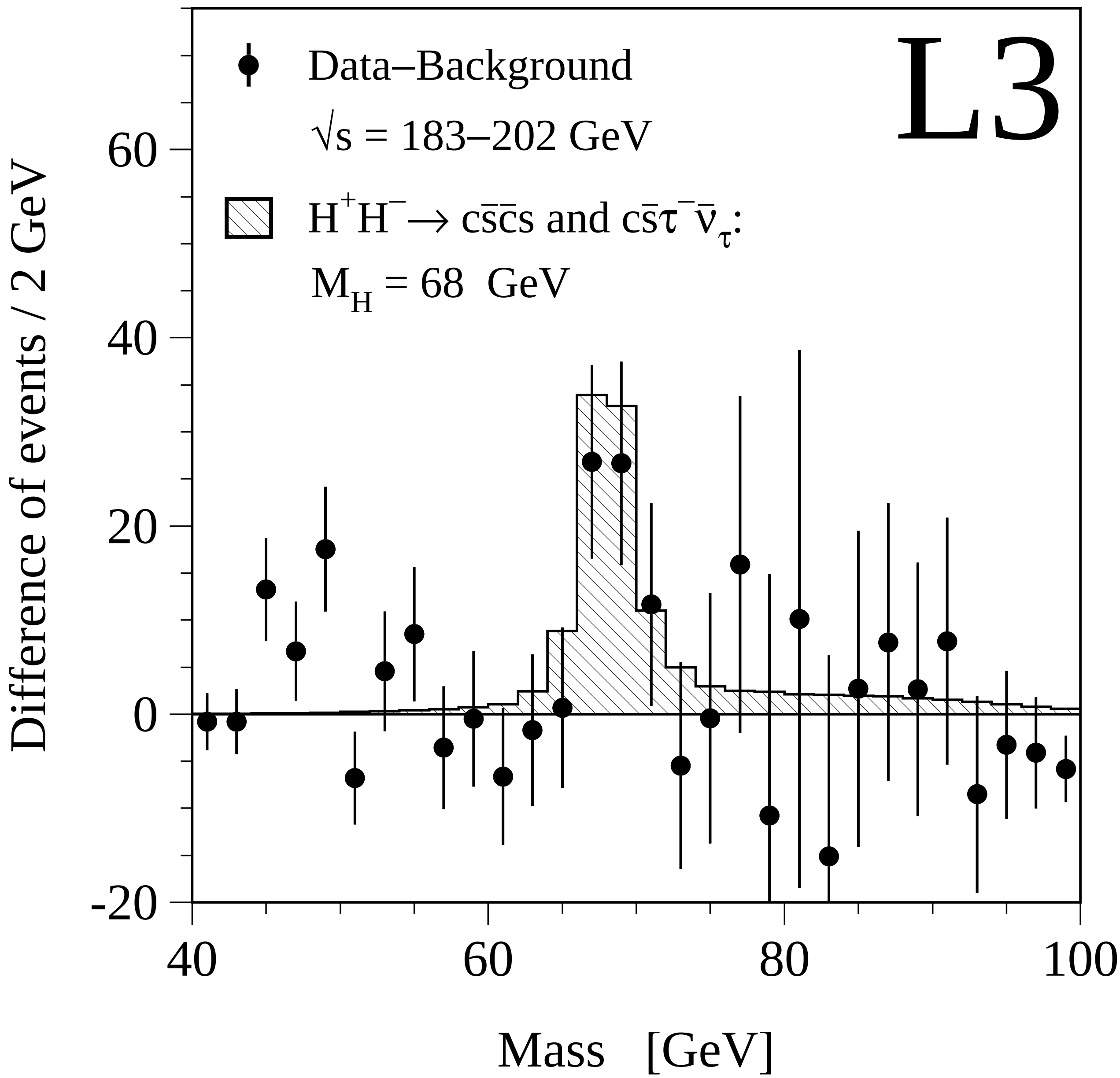

Figure 4: Combined background-subtracted mass distribution for the $H^+H^- \rightarrow c\bar{s}\bar{c}s$ and $c\bar{s}\tau^-\bar{\nu}_\tau$ decay channels, where the events are corrected for the efficiency of their respective analyses. The expected distribution for a 68 GeV Higgs with $Br(H^\pm \rightarrow \tau\nu) = 0.1$ is shown by the hatched histogram.

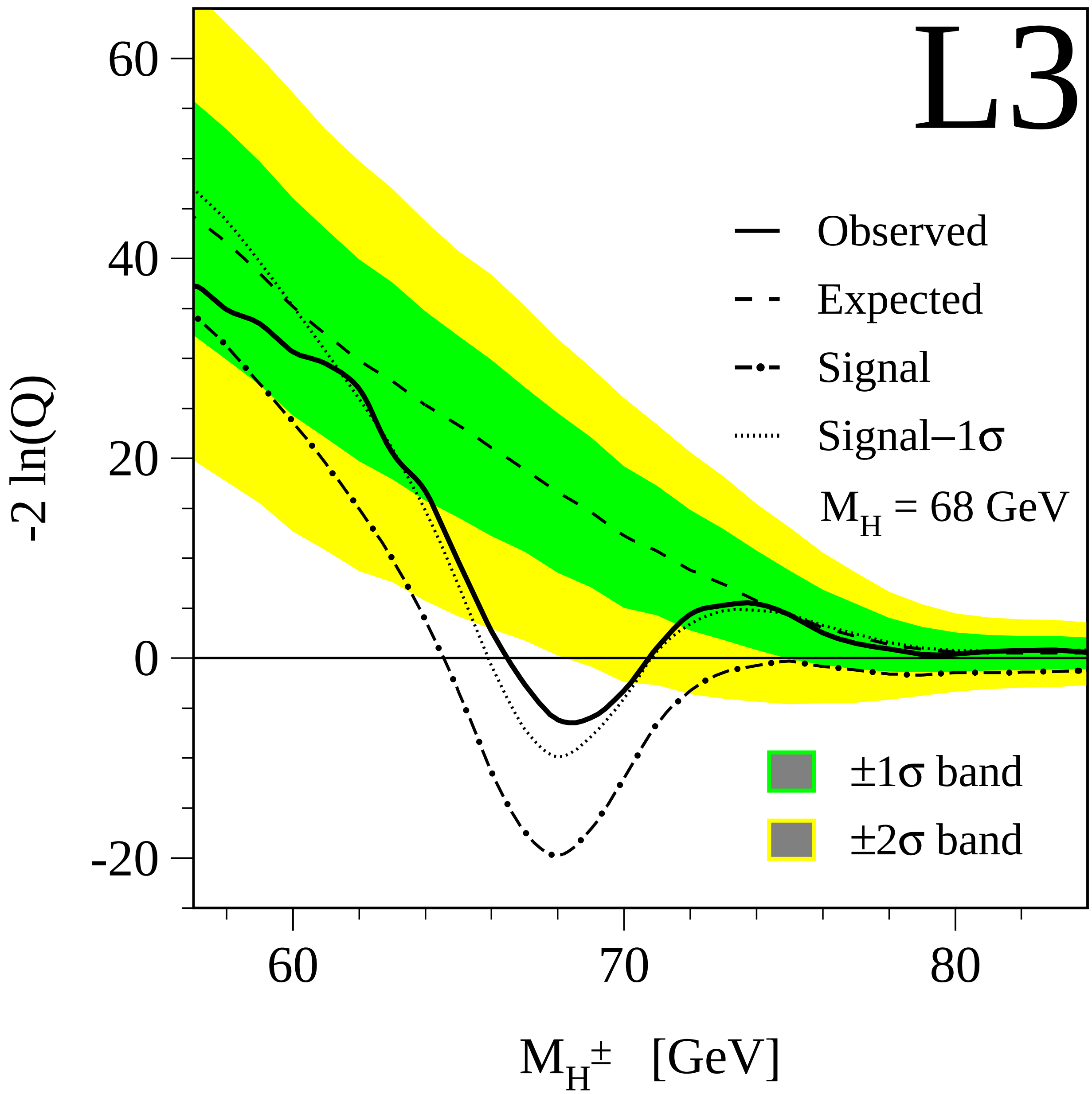

Figure 5: The negative log-likelihood ratio, $-2\ln(Q)$, as a function of the Higgs mass with $\mathrm{Br}(\mathrm{H}^{\pm} \rightarrow \tau\nu) = 0.1$. The solid line shows the values computed from the observed results and the dashed line the expectation for the background only hypothesis. The dash-dotted line is the curve expected for a 68 GeV Higgs signal at this value of the branching ratio. The dotted line is the expected result for a 1σ under-fluctuation of the signal. The shaded areas represent the symmetric 1σ and 2σ probability bands expected in the absence of a signal.

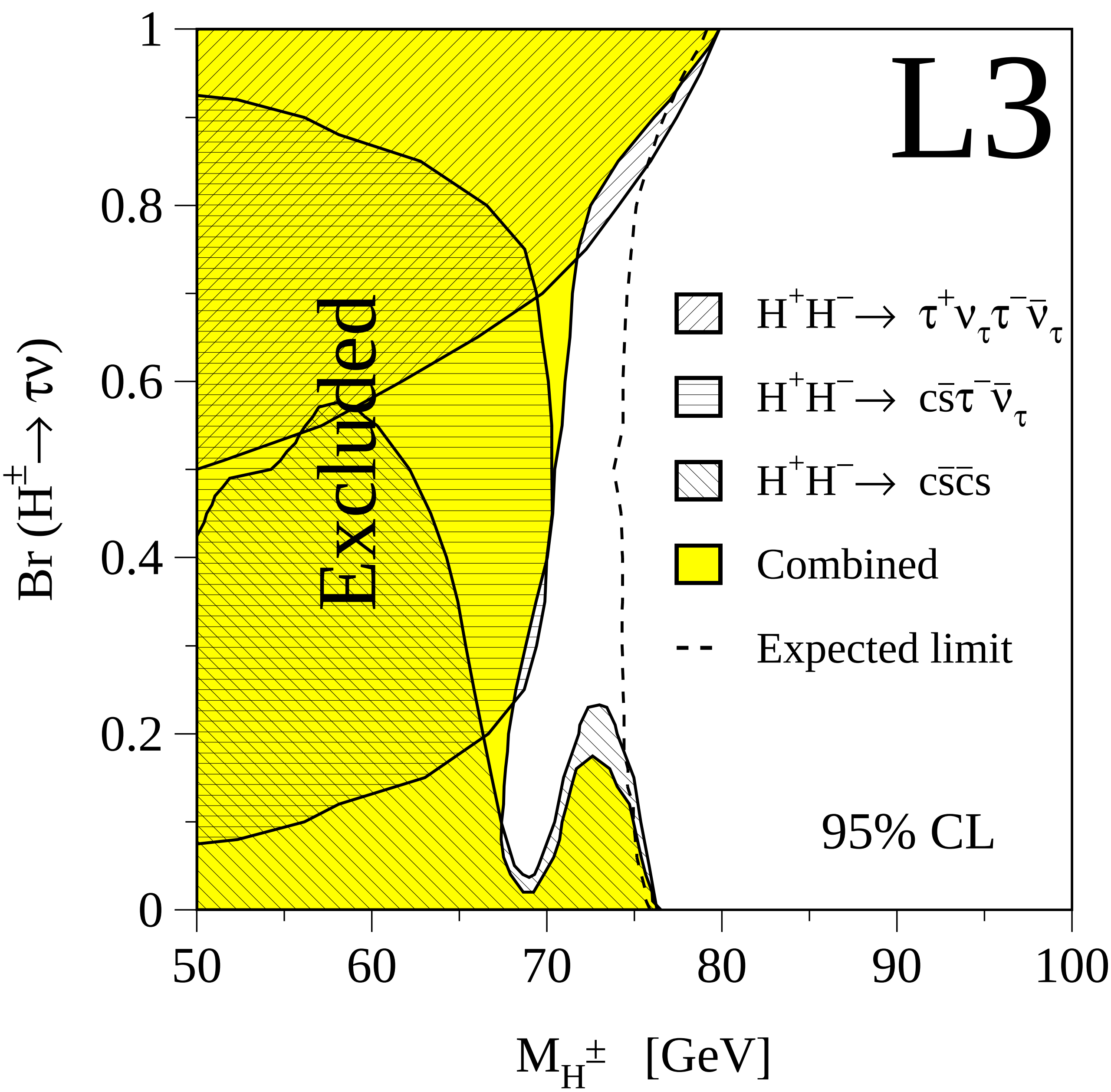

Figure 6: Excluded regions for the charged Higgs boson at more than 95% CL in the plane of the $H^\pm \to \tau\nu$ branching fraction versus mass, for the analyses of each final state and their combination. The dashed line indicates the median expected limit in the absence of a signal. There are regions excluded by the individual analyses but not by their combination.